Article type : Technical Paper

Comparative Analysis of Inundation Mapping Approaches for the 2016 Flood in the Brazos River, Texas

Jiaqi Zhang, Yu-Fen Huang, Dinuke Munasinghe, Zheng Fang, Yin-Phan Tsang, and Sagy Cohen

Graduate Student (**Zhang**) and Assistant Professor (**Fang**), Department of Civil Engineering, University of Texas at Arlington, Rm 431, Nedderman Hall, 416 Yates St., Arlington, Texas 76019; Graduate Student (**Huang**) and Assistant Professor (**Tsang**), Department of Natural Resources and Environmental Management, University of Hawaii at Manoa, Honolulu, Hawaii 96822; Graduate Student (**Munasinghe**) and Assistant Professor (**Cohen**), Department of Geography, University of Alabama, Tuscaloosa, AL 35487 (E-Mail/Fang: nickfang@uta.edu).

Abstract: Accurate and timely flood inundation maps serve as crucial information for hydrologists, first-responders and decision makers of natural disaster management agencies. In this study, two modeling approaches are applied to estimate the inundation area for a large flooding event occurring in May of 2016 in the Brazos River: (1) Height Above the Nearest Drainage combined with National Hydrograph Dataset Plus (NHDPlus-HAND) and (2) International River Interface Cooperative— Flow and Sediment Transport with Morphological Evolution of Channels (iRIC-FaSTMECH). The inundation extents simulated from these two modeling approaches are then compared against the observed inundation extents derived from a

This is the author manuscript accepted for publication and has undergone full peer review but has not been through the copyediting, typesetting, pagination and proofreading process, which may lead to differences between this version and the Version of Record. Please cite this article as doi: 10.1111/1752-1688.12623-17-0035

Landsat-8 Satellite image. The simulated results from NHDPlus-HAND and iRIC- FaSTMECH show 56% and 70% of overlaps with the observed flood extents, respectively. A modified version of the NHDPlus-HAND model, considering networked catchment behaviors, is also tested with an improved fitness of 67%. This study suggests NHDPlus-HAND has the potential for real-time continental inundation forecast due to its low computational cost and ease to couple with the NWM. Better performance of NHDPlus-HAND can be achieved by considering the inter-catchment flows during extreme riverine flood events. Overall, this study presents a comprehensive examination made of remote sensing compared with HAND-based inundation mapping in a region of complex topography.

(**Key Terms**: Flooding; Inundation; NHDPlus-HAND; iRIC; Simulation; Observation; Remote Sensing.)

INTRODUCTION

Flooding is one of the leading causes of natural disaster related deaths worldwide (Federal Emergency Management Agency, 1992; Conrad *et al.*, 1998; Merwade *et al.*, 2008; Cook and Merwade, 2009). According to a study on flood damage in the United States, flood damage increases over time due to rapidly growing population and urban development (Pielke *et al.*, 2002). Accurate and timely inundation maps not only provide first-hand information for rescuing and emergency operations during floods, but also potentially improve flood risk management and better estimate flood insurance rates (Merwade *et al.*, 2008; Cook and Merwade, 2009; Fang *et al.*, 2011). In the United States, most major river systems have flood-risk maps delineated by the Federal Emergency Management Agency (FEMA) through the National Flood Insurance Program (NFIP). Although FEMA has produced approximately 100,000 flood-risk maps based on 100-year return period flows (NFIP, 2002), inundation maps for real events are unavailable or limited by uncertainties in data sources or modeling (Christian *et al.*, 2013).

Flood inundation modeling approaches are essentially to convert flows from either hydrologic models or observation gages into inundation extent/depth based upon topographic information. In general, inundation models can be classified as terrain-based and dynamic-based approaches. Terrain-based approaches refer to the methods employing topography and simplifying the fluid mechanics process to predict inundation extents. Intersecting topography surface with a planar water surface is normally defined as the simplest terrain-based approach to generate inundated area (Priestnall *et al.*, 2000). Some terrain-based models are also known as storage cell models by treating the floodplain as many storage cells and solving uniform flow formulas like Manning's and weir-type equations for floodplain routing (Cunge *et al.*,1976; Estrela, 1994; Romanowicz *et al.*, 1996, Bates and De Roo, 2000). Another type of terrain-based approach calculates the elevation difference between each grid cell and its nearest flowpath grid based on topographic information (Nobre *et al.*, 2011). In summary, the terrain-based approaches aim to reduce computational cost while generating satisfactory inundation results.

Dynamic-based approaches include hydraulic/hydrodynamic models which are generally categorized as one-, two- and three-dimensional models. One-dimensional hydraulic models consider fluid continuity and momentum, which solve one-dimensional St. Venant equations. One example of such hydraulic models is the Hydrologic Engineering Center's River Analysis System (HEC-RAS) developed by the U.S. Army Corps of Engineers (USACE). The general steps of inundation mapping using one-dimensional hydraulic models involve: (1) obtaining discharge information from gage observation or a calibrated hydrologic model; (2) developing perpendicular cross sections along the flow path based on Digital Elevation Model (DEM) or survey information with hydraulic parameters (e.g. surface roughness); (3) calculating the water surface elevations based on the discharge and cross-sectional information from the previous steps; (4) comparing the water surface elevations with DEMs, and the area where water surface is higher than terrain elevation is defined as inundated (IACWD 1982; Maidment and Djokic, 2000; Noman *et al.*, 2001; FEMA 2003; Merwade *et al.*, 2008). Two-dimensional hydraulic models use finite-element mesh as a calculation unit and have capability to simulate the lateral unsteady flow dynamics including backflow condition (Crowder and Diplas, 2000; Merwade *et al.*, 2008). Three-dimensional hydraulic models can fully represent the comprehensive form of the Navier-Stokes equations (White, 1974; Lane *et al*, 1999). Since three-dimensional approaches might be unnecessarily complex and computationally expensive (Bates and De Roo, 2000; Horritt and Bates, 2001; Hunter *et al.*, 2007), one- and two-dimensional models are the primarily used in floodplain prediction to date (Hunter *et al.*, 2007). Table 1 shows the comparison between dynamic-based and terrain-based inundation mapping approaches.

[INSERT TABLE 1 HERE]

[Table 1. Comparison of dynamic-based and terrain-based inundation approaches]

Height Above the Nearest Drainage combined with National Hydrograph Dataset Plus (NHDPlus-HAND) is a terrain-based flood indundation model. The Height Above the Nearest Drainage (HAND) concept was first introduced by Rennó *et al*. (2008). The HAND model normalizes topography based on relative heights found along the nearest drainage network (Nobre *et al*., 2011). The HAND raster is generated by subtracting the elevation of each grid cell from the elevation of its nearest stream grid cell. Nobre *et al.* (2016) has validated the HAND method using a flood event in Southern Brazil with a finding that HAND can be used to predict inundation extents. Since HAND rasters are computed based on topography and flowpath information, accurate Digital Elevation Model (DEM) and flowline are essential components in establishing a HAND model. The National Hydrograph Dataset Plus (NHDPlus) is an integrated geo-spatial, hydrologic dataset built by the U.S. Environmental Protection Agency (USEPA) Office of Water and the US Geological Survey (USGS). The NHDPlus Version 2 dataset provides a reliable stream network consisting of approximately 2.7 million reaches in the continental United States (http://www.horizon-systems.com/nhdplus/). Liu *et al*. (2016) calculated HAND rasters for the contiguous United States using a 10-m resolution DEM combined with NHDPlus streamlines (termed NHDPlus-HAND). For delineating inundation maps, HAND needs discharge and rating curve information from hydrologic/hydraulic models. Brought into operations in August of 2016, the National Water Model (NWM) is a high-resolution hydrologic model simulating discharge for 2.7 million NHDPlus (Version 2) stream reaches over the continental United States (NOAA, 2016). The NWM is developed based on the Weather Research and Forecasting Model Hydrological (WRF-Hydro) framework, which utilizes meteorological forcing from the operational High Resolution Rapid Refresh (HRRR) model and precipitation forcing from the Multi-Radar/Multi-Sensor System (MRMS). To obtain discharge information, the NWM utilizes a vector-based channel routing module based on the NHDPlus reaches, which was firstly demonstrated using the Routing Application of the Parallel Computation of Discharge (RAPID) in 2015 (Maidment, 2017; Lin *et al*., 2017), and then evolved into the Muskingum-Cunge routing method in 2016 (NOAA, 2016). This study uses a set of the pre-operational NWM discharge data that ingests the streamflow data assimilation capability at ~7000 gauge stations (NOAA, 2016) on top of the Muskingum-Cunge routing. The NHDPlus-HAND is chosen as the terrain-based model for the study due to its ease of application to be coupled with the existing hydrologic model (NWM).

A dynamic-based model, International River Interface Cooperative - Flow and Sediment Transport with Morphological Evolution of Channels (iRIC-FaSTMECH) is a two-dimensional hydrodynamic model employing a channel-fitted coordinate system (cylindrical coordinate system), where the curvature follows the stream direction (FaSTMECH Model Note. Accessed March 1, 2017, http://i-ric.org/en/downloads). It provides information of velocity and water surface elevation for a given discharge and roughness by hydrostatic-distribution pressure and a quasi-steady approximation (Nelson and McDonald, 1996), which allows the discharges to vary in time, and simplifies unsteady terms in the equations of motion. The iRIC system includes different models with less restrictive assumptions and more applicability but requires more extensive calibration data (Nelson *et al*., 2016, www.i-ric.org). The iRIC model framework is upgraded from the Multi-Dimensional-Surface Water System Modeling System (MD-SWMS) (McDonald *et al*., 2001, 2005), which employs a finite difference approach on a curvilinear grid to solve the depth and Reynolds-averaged Navier-Stokes equations (Nelson *et al*., 2003). Not only can the iRIC-FaSTMECH provide the maximum inundation area at peak stage but also be used for simulating water level, flow velocity distribution for the floodplain, etc. (Ku and Kim, 2014; Son *et al*., 2014; Kail *et al*., 2015). Kenney and Freeman (2011) suggested that iRIC-FaSTMECH give a fair spatial understanding of water-surface elevation, velocities, and sheer stress associated with high flows. Son *et al*. (2014) showed that iRIC-FaSTMECH well simulated water-surface levels in South Korea. Due to its simulation efficiency and utility in predicting water-surface elevation during the flood event, iRIC-FaSTMECH is selected as the dynamic-based model in this study.

Lack of reliable observed spatial extents of flood inundation limits the validation and utility of both approaches in flood inundation mapping. Fortunately, the advent of satellite-based remote sensing technology has become a key tool for flood monitoring (e.g. Dartmouth Flood Observatory: http://floodobservatory.colorado.edu). Such applications of satellite imagery for river inundation (e.g. the U.S. Flood Inundation Map Repository: http://sdml.ua.edu/usfimr) serve as observations on flooding areal extents within the region of interest (Khan *et al*., 2011).

In this regard, the authors are motivated to investigate the performances of various inundation simulations based on observation derived using remote sensing techniques. A better understanding of mechanisms of terrain- and dynamic-based inundation approaches can then be achieved. Furthermore, deeper insights are gained to improve the timeliness and accuracy of real-time flood inundation mapping. This study is conducted to achieve the following objectives:

1. To validate the NHDPlus-HAND's simulation using streamflow information from the NWM along with the observation derived from the satellite imagery.

2. To evaluate the terrain-based (NHDPlus-HAND) and dynamic-based (iRIC-FaSTMECH) models with respect to modeling accuracy, modeling efficiency (running time), and feasibility in real-time mode.

3. To provide suggestions for future model development and explore potential efficient ways to improve NHDPlus-HAND towards accurate large-scale inundation mapping.

STUDY AREA

Based on a request for presidential disaster declaration by Abbott (2016), 12 counties in Texas with a population of 3.9 million were impacted by a flood event occurring in the Brazos River in May of 2016. There were over 11,000 people evacuated from their impacted homes along the Brazos River (Abbott, 2016). Due to the severity of the flood, the May of 2016 event is particularly selected for this study to seek useful information for future decision making under severe weather conditions.

The study area (Figure 1) is a section of the Brazos River spanning 27 km of main-stem distance upstream of the USGS gage near Hempstead (ID: 8111500). The inundation of the May 2016 event over the study area was captured in a relatively cloud-free Landsat 8 image. As shown in Figure 2B, the majority of the area appears to be flooded in comparison with the pre-flood condition (Figure 2A). The USGS gage (ID: 8111500) recorded a total rainfall of 255.8 mm within 25 hours, as well as the peak stage of 16.78 m (above the datum) at 3 p.m. on May 27th, 2016 (CDT). The Landsat 8 imagery (Figure 2B) was captured at 12 p.m. on May 28th (CDT), 21 hours after the peak stage occurred. However, at the moment when satellite imagery was taken, it shows that the stage elevation decreased from the peak stage elevation only by 2.5% (Figure 3), implying the slow recession of the river after the peak stage occurred. Because of such a small difference, the flood extents captured by satellite imagery is assumed to represent the peak inundation in this study.

[**INSERT FIGURE 1 HERE**]

[Figure 1. The study area and stream reaches in the Brazos River, Texas]

[**INSERT FIGURE 2 HERE**]

[Figure 2. Satellite imageries showing A. pre-flood (12 p.m. on March 25th, 2016(CDT)) and B. post-flood condition (12 p.m. on May 28th, 2016(CDT)) in the study area]

[INSERT FIGURE 3 HERE]

[Figure 3. Stage hydrograph and rainfall hyetograph shows the target timing of model simulation and the timing of satellite observation]

METHODOLOGY

To better understand and evaluate two inundation modeling methods and their corresponding performances, the authors conduct a series of comparisons of simulated inundation from both approaches, i.e. terrain-based (NHDPlus-HAND and the modified HAND) and dynamic-based (iRIC-FaSTMECH), with observed inundation from the satellite imagery for the study area during the May 2016 event. For simplicity, NHDPlus-HAND and iRIC-FaSTMECH are referred to as HAND and iRIC respectively in the following sections. The methodology consists of three major parts: HAND, iRIC, and remote sensing. The HAND model uses hydrologic model's outcome as the input discharge to delineate flood inundation. As a supplementary approach, a modified version of HAND is also tested for inundation mapping. The iRIC is a two-dimensional hydraulic model, to simulate flood inundation maps. Satellite imagery is used as observation for further comparisons with simulations in the third part. Figure 4 illustrates the data and workflow of the methodology with more details in the following sections.

[**INSERT FIGURE 4 HERE**]

[Figure 4. Schematic diagram of this study]

NHDPlus-HAND

NHDPlus-HAND generates inundation maps through the procedure as shown in Figure 4. First, the NWM output provides hourly discharge information for each NHDPlus flowline (identified by a unique ID number - ComID). In general, the discharge from the NWM undergoes nudging-based data assimilation wherever/whenever gage-observed values become available, which leads to a close match between the NWM discharge and observed discharge as shown in Figure 5. Then these NWM flow information is converted into stage height using rating curves (stage-discharge relationship). The rating curve for each reach is generated from channel properties in the HAND model based on Manning's equation. These interpreted stage height information allows us to determine inundation extents from the HAND raster. In each catchment, HAND cells with lower elevation than the interpreted stage height information can be classified as 'wet' cells. For example if the calculated stage for a given catchment (ComID) is 5 m, all HAND cells with a value between 0 and 5 will be classified as 'wet' cells. A simple GIS-based Raster Calculator equation is applied to identify the 'wet' cells. The whole methodology of creating inundation map using HAND is automated with a Python script utilizing a number of ArcGIS tools for a better efficiency.

[**INSERT FIGURE 5 HERE**]

[Figure 5. U.S. Geological Survey gage observed hydrograph and the National Water Model hydrograph with nudging-based data assimilation]

Modified HAND

The NHDPlus-HAND method typically enables users to determine inundated area based on individual NHDPlus catchment with corresponding water depth. However, with the assumption of applying uniform water depth for each catchment, NHDPlus-HAND cannot consider inter-catchment flow mechanisms, i.e. the flow transfer between adjacent catchments. To tackle this deficiency, McGehee *et al*. (2016) developed the modified HAND method by taking stream orders into account when determining the nearest drainage. In essence, the modified HAND method provides an approach to re-define channel network, i.e. deleting streams with low stream orders. McGehee *et al*. (2016) stated that such a modification, if applied locally where the original HAND overlooks catchment interaction, can potentially improve the accuracy of inundation mapping (as demonstrated later). Therefore, the modified HAND method is used to improve the HAND simulation in this study and compare with other inundation mapping results.

iRIC-FaSTMECH

The terrain used to develop iRIC-FaSTMECH model is 10-meter resolution DEM obtained from USGS database (https://earthexplorer.usgs.gov), and the NHDPlus-HAND is developed using DEM of the same resolution (10 meters). Table 2 shows the final model settings for generating inundation by iRIC, and specific procedures are illustrated in Figure 4. The researchers first assign a water surface elevation as the initial upstream condition and the peak discharge (4,445.7 m^3/s) with stage information (49.7 m) from USGS gage (8111500) as the downstream boundary condition, respectively. After numerous iterations, the iRIC model is able to compute a converged solution as upstream discharge (4,300 m^3/s). During the iterations, drag coefficient is updated as it is a function of Manning's coefficient and water depth which varies with upstream discharge. Three Manning's coefficients (0.03, 0.05 and 0.035) are used to corresponding land cover types (main channel, brushy and cultivated) (Chow 1959). Finally, inundation maps are delineated using the optimal drag coefficient and discharge after 1,500 iterations. Suggested by Nelson (2016), re-wetting option is turned during the modeling process on since it can improve inundation estimations in large and shallow areas by re-evaluating the wet/dry status of each node during the simulation.

[INSERT TABLE 2 HERE]

[Table 2. iRIC model settings]

Satellite-based Flood Inundation Mapping

Landsat Satellite missions have been applied in delineating floodplain boundaries over a few regions under different conditions in climate, morphology and land use since 1972 (Rango *et al.*, 1975; Hollyday, 1976; Sollers *et al.*,1978; Smith, 1997; Ho *et al.*, 2010). Amongst the many different techniques of identifying water pixels using a suite of the Landsat Satellites, Supervised Classification has been proven as a robust method to classify features of interest (Frazer and Page, 2000; Shalaby and Tateishi, 2007). The Supervised Classification technique allows users to select sample pixels (end members) in an image as representatives of a specific spectral signature (e.g. water). Image processing software is then used to classify all the image pixels based on the maximum likelihood that these pixels' spectral signature is similar to that of a specific end member.

The remote sensing imagery used in this study is obtained from the Landsat 8-Operational Land Imager (OLI) multispectral database (http://earthexplorer.usgs.gov). The pre-flood (March 25, 2016) and post-flood (May 28, 2016) images are classified via Erdas Imagine® 2015 Image processing software (Hexagon Geospatial, Norcross, GA, USA) for pre-processing and subsequent data manipulation. The resultant Geometrically and Radiometrically rectified imagery is subject to Supervised Classification of flooded pixels based on the maximum likelihood classifier. Typically, the presence of clouds is a common problem in remote sensing imagery, which hinders the identification of flooded water pixels beneath the clouds, leading to under-representation of flood water extents in the study domain. In an attempt to alleviate this problem, the DEM of the flooded region is used to identify the height of the pixels beneath the clouded areas. Each pixel with a lower height than that of the lowest height of an apparent flooded pixel in the neighborhood of the cloud is considered as 'wet'. Spatial filling techniques are then applied to convert these pixels into water pixels. Accuracy assessments are finally performed on the classified imagery subsequent to being post-processed through a 3×3 high pass kernel (Zhang *et al*., 2016). A high pass kernel has the effect of highlighting boundaries between features (e.g., where water body meets the vegetated land), thus water features can be easily classified by sharpening edges between water and non-water pixels.

Advanced Fitness index (AFI)

In order to evaluate the correspondence between the simulated and observed inundation, the advanced fitness index (AFI) method is applied in this study. The AFI accounts for the match in terms of both inundated and non-inundated area, as shown in **Equation 1**:

$$\text{Advanced Fitness (\%)} = \frac{IA_{obs} \cap IA_{model} + NIA_{obs} \cap NIA_{model}}{A_{total}} \times 100 \qquad (1)$$

where IA_{obs} /NIA_{obs} is inundated/non-inundated area of the observation; IA_{model}/NIA_{model} is inundated/non-inundated area of the model simulation, and A_{total} is the total area of the study region.

The simulated and observed inundation results cannot be compared directly because of their different resolution and patchy nature of the classified water body in a satellite image. To tackle this technical difficulty, the simulated inundation is further resampled to 30 m x 30 m grids and aligned to be consistent with the observed. To evaluate the mapping performances based on corresponding AFI values, the raster calculator function in ArcGIS is used to quantify the inundated/non-inundated area with number of pixels. The following section demonstrates the results from aforementioned methods with an evaluation on their performances.

RESULTS AND DISCUSSION

Inundation maps for the 2016 May flood event in the Brazos River using terrain-based, physical modeling methods and remote sensing classification technique are shown in Figures 6A, 6B, 6C and 6D, respectively. In general, inundation areas derived from the iRIC and modified HAND methods have more overlaps with the observed inundation than the original HAND simulation. Also, the HAND simulation clearly misses a few areas considered inundated by all other two methods. As the advanced fitness indices (AFI) indicated, the HAND model has a 56% match with the observation, while iRIC and the modified HAND have higher AFI values of 70% and 67%, respectively. The modified HAND appears to delineate larger inundated area than iRIC, but still generates inferior AFI. As a supplementary approach to HAND, the modified HAND method is found to improve the AFI value by 11% with capturing a few missed areas. Interestingly, the inundation classified from satellite imagery has the least area of only 41.3 km^2, compared to the other three modeling approaches (55.9 km^2 for iRIC, 41.7 km^2 for HAND and 70.8 km^2 for modified HAND). Although as shown in Figure 6D, the inundated area appears to have some discontinuous features or gaps, leading to the reduced inundation area, the authors consider the inundation from satellite imagery as the 'true' flooded area during the study.

[**INSERT FIGURE 6 HERE**]

[Figure 6. Results of inundation maps and fitness indices from simulation of (A) HAND, (B) iRIC, (C) Modified HAND, and (D) Satellite Observation]

Further investigation is performed to discover why HAND misses certain areas that are captured by the other two methods. Compared to HAND (Figures 7A and 7B), an in-depth illustration for the improvement of the modified HAND simulation is shown in Figures 7C and 7D. The left two panels (7A and 7C) respectively show inundated areas of the HAND and modified HAND simulations on top of the topography. The two highlighted NHDPlus catchments 1 and 2 are chosen to exemplify the difference between the HAND and modified HAND methods. It is found that discrepancy between the results of two methods mainly takes place in catchment 2. Catchment 1 is located along the Brazos River main stem with a higher stream order than that of catchment 2 which drains into the main stream as tributary. The cross-sectional views of selected cutting line across catchment 1 and 2 with corresponding simulated water surface elevation (blue lines in the right panels) are shown in Figures 7B and 7D, respectively. The disconnected water surface shown in Figure 7B indicates that the catchment-based calculation by HAND overlooks the inter-catchment flow. However, the water surface would be more realistically simulated as shown in Figure 7D if the modified HAND is strategically applied to the problematic areas. Therefore, the results show that the modified HAND can essentially replace the water depth of the low-stream-order catchment (catchment 2 herein) with that of the adjacent catchment with high stream order (catchment 1), instead of determining the inundation of the catchments based on their individual water depth solely.

[**INSERT FIGURE 7 HERE**]

[Figure 7. (A) Inundation map derived from HAND on top of DEM, (B) Cross-sectional view of the selected area and water surface simulated in HAND, (C) Inundation map derived from the modified HAND on top of DEM, (D) Cross-sectional view of the selected area and water surface simulated in modified HAND]

Overall, iRIC is found to generate the best match with the observation in this case study. Bates and De Roo (2000) also reported in their study that two-dimensional models would perform better than terrain-based models when their resolution was similar. If the problematic catchments in HAND simulation are excluded from the comparison, the HAND and iRIC models would generate comparable AFI values (65% and 68% respectively). Such results indicate that aside from HAND's deficiency to model inter-catchment inundation, it has equivalent capability as iRIC in terms of matching the observation. This study suggests that simplification on the intricacy of flow dynamics employed by terrain-based models has relatively minor influence on peak inundation prediction. This finding confirms that using a simple terrain-based model could adequately simulate the flood inundation area as discovered by Bates and De Roo (2000).

Although the dynamic-based model represented by iRIC in this study provides more accurate estimates under high flow conditions, the model needs intensive calibrations using various historical data to achieve a reliable performance (Nobre *et al*., 2016). Promisingly, terrain-based model, as represented by HAND in this study, demonstrates a unique inundation mapping capability for a river section without much historical data. Given the fact that solving the St.Venant equations for hydraulic/hydrodynamic models through iterating process is very computationally expensive, their utility is limited in real-time flood prediction (Fang *et al.*, 2008). In our case, the iRIC model needs approximately 90 minutes (5,400 seconds) to run 1,500 iterations, while the HAND model only takes about 2 minutes (120 seconds) for 37 NHDPlus river reaches to generate the inundation. For a large-scale hydrologic forecasting system like the NWM, the HAND inundation mapping approach clearly shows benefits in coupling with the model as demonstrated in this study, potentially addressing the real-time continental-scale inundation mapping problem in an efficient way.

However, the HAND calculation does not explicitly reflect interactions between the main stem and its tributaries. This issue likely becomes more pronounced for larger riverine floods. In addition to the modified HAND, one remedy to this problem is to incorporate a mass balance process into the modeling framework as suggested by Bates and De Roo (2000). The authors think that while not observed in this study, the accuracy of the HAND model would be inferior to a traditional hydraulic model if the flooded area has complex urban hydraulic components like culverts, pipes and bridges. Therefore, extra caution should be taken when choosing proper inundation models for flood risk prediction due to the uncertainties in data requirement, computation demand, accuracy, types of land cover, etc.

CONCLUSIONS AND FUTURE WORK

This paper demonstrates a unique analysis of using terrain-based (NHDPlus-HAND and the modified HAND) and physical (iRIC-FaSTMECH) models to simulate the maximum inundation extents during the May 2016 flood event in the Brazos River, TX. A supervised classification method is used to classify water from Landsat 8 satellite imagery and generate an observed inundation map. To better understand and evaluate the performances of three methods, the goodness of overlapping between the simulated and observed is quantified via the advanced fitness index (AFI). The main conclusions from this study are summarized as follows:

1. NHDPlus-HAND, the modified HAND and iRIC generated a fair (> 50% of AFI) fit with the satellite imagery. iRIC performed a slight better (~ 70% in AFI) than other two methods (NHDPlus-HAND and the modified HAND) during this extreme flood event.

2. Although the NHD catchment-based calculation does not allow NHDPlus-HAND to explicitly account for inter-catchment flows between the main stem and its tributaries, the modified HAND method provides a remedy to this issue when strategically applied to the areas overlooked by NHDPlus-HAND.

3. For extreme events, simplification on the intricacy of flow dynamics has relatively minor influence on predictions, which can positively justify the utility of NHDPlus-HAND for large-scale inundation mapping.

4. Even though the current version of NHDPlus-HAND may not be a superior choice for handling accurate inundation mapping for urban areas, its low computational cost and ease to couple with the National Water Model (NWM) provide great potential to support real-time continental inundation forecast in the future.

The authors think that there is room for future investigation in uncertainty analysis of observations using multiple sources of raw imagery along with various classification techniques. Potential sources of raw imagery will be used including synthetic aperture radar (SAR), unmanned aerial vehicle (UAV) and so on; while classification methods like Delta-cue change detection on pre/during flooding scenarios, normalized difference water index and image fusion techniques will be also used to generate inundation extents. The results of the future research will be reported in a forthcoming paper.

Overall, this study presents a comprehensive examination made of remote sensing compared with HAND-based inundation mapping in a region of complex topography. Findings from this paper can also help identify potential improvements for HAND-based simulation. In light of frequent floods occurring in the nations, the information provided from this study is valuable for the scientific/engineering communities, floodplain managers, emergency personnel and governmental entities that were impacted by the storm and/or had a vested interest in the region.

ACKNOWLEDGMENTS

This research was conducted during the 2016 NOAA National Water Center (NWC) Summer Institute administered by the Consortium of Universities for the Advancement of Hydrologic Science, Inc. (CUAHSI). The authors would like to thank Peirong Lin and Adnan Rajib for their coordination and all the advisory faculty, theme leaders and coordinators involved in the 2016 Summer Institute. The authors would especially like to thank, Dr. David Maidment, Dr. Sarah Praskievicz and Dr. Richard McDonald for their generous support and thoughtful comments during the period of our project work. Fang and Zhang would like to thank the Tarrant Reginal Water District (TRWD) and the National Science Foundation (NSF) under Grant No. CyberSEES-1442735 for their support. Tsang and Huang would like to thank Dr. Yi-Leng Chen for his assistance to the workshop travel and application. Cohen and Munasinghe would like to thank the University Corporation for Atmospheric Research (UCAR) and the NWC for their support via the COMET Program Cooperative Project Grant under Cooperative Agreement No. Z16-23487 with the National Oceanic and Atmospheric Administration (NOAA).

LITERATURE CITED

Abbott, G., 2016. Request for Presidential Disaster Declaration — Major Disaster. http://gov.texas.gov/files/press-office/FederalDisasterRequest_06092016.pdf

Bates, P.D., M.G. Anderson, L. Baird, D.E. Walling, and D. Simm, 1992. Modelling Floodplain Flow with A Two-Dimensional Finite Element Scheme. *Earth Surface Processes and Landforms* 17: 575–588. DOI: 10.1002/esp.3290170604

Bates, P.D. and A.P.J. De Roo, 2000. A Simple Raster-based Model for Flood Inundation Simulation. *Journal of Hydrology* 236(1): 54-77. DOI: 10.1016/S0022-1694(00)00278-X

Chow, V.T., 1959. Open Channel Hydraulics. McGraw-Hill Book Company, Inc; New York, ISBN-13: 978-0070107762

Christian, J., L. Duenas-Osorio, A. Teague, Z. Fang, and P. Bedient, 2013. Uncertainty in Floodplain Delineation: Expression of Flood Hazard and Risk in A Gulf Coast Watershed. *Hydrological Processes* 27(19): 2774-2784. DOI: 10.1002/hyp.9360

Cook, Aaron and Venkatesh Merwade, 2009. Effect of Topographic Data, Geometric Configuration and Modeling Approach on Flood Inundation Mapping. *Journal of Hydrology* 377(1): 131-142. DOI: 10.1016/S0022-1694(00)00177-3

Crowder, D.W. and P. Diplas, 2000. Using Two-dimensional Hydrodynamic Models at Scales of Ecological Importance. *Journal of Hydrology* 230(3): 172-191. DOI: 10.1016/S0022-1694(00)00177-3

Conrad, D., M. Stout, and B. McNitt, 1998. Higher Ground: A Report on Voluntary Property Buyouts in the Nation's Floodplains. *National Wildlife Federation*, Vienna, Va.

Cunge, J.A., F.M. Holly, and A. Verwey, 1976. Practical Aspects of Computational River Hydraulics. Pitman, London, ISBN-13: 978-0273084426

Estrela, T., 1994. Use of A GIS in the Modelling of Flows on Flood-plains. In: *Proceedings of the 2nd International Conference on River Flood Hydraulics*, White, W.R. and J. Watts (Editors). Wiley, Chichester, UK, Vol. 177, p. 190.

Fang, Z., P.B. Bedient, J. Benavides, and A.L. Zimmer, 2008. Enhanced Radar-Based Flood Alert System and Floodplain Map Library. *Journal of Hydrologic Engineering* 13(10): 926-938. DOI: 10.1061/(ASCE)1084-0699(2008)13:10(926)

Fang, Z., P.B. Bedient, and B. Buzcu-Guven, 2011. Long-Term Performance of A Flood Alert System and Upgrade to FAS3: A Houston, Texas, Case Study. *Journal of Hydrologic Engineering* 16(10): 818-828. DOI: 10.1061/(ASCE)HE.1943-5584.0000374

Federal Emergency Management Agency (FEMA), 1992. Floodplain Management in the United States: An Assessment Report. *Federal Interagency Floodplain Management Task Force*, prepared by L. R. Johnston Associates.

Federal Emergency Management Agency (FEMA), 2003. Guidelines and Specifications for Flood Hazard Mapping Partners, Appendix C: Guidance for Riverine Flooding Analysis and Mapping. http:// www.fema.gov/pdf/fhm/frm_gsac.pdf.

Frazier, P.S. and K. J. Page, 2000. Water Body Detection and Delineation with Landsat TM Data. *Photogrammetric Engineering and Remote Sensing* 66(12): 1461-1468. DOI: 10.1109/Argo-Geoinformatics.2013.6621909

Fread, D.L., 1984. In: *Hydrological Forecasting*, Anderson, M.G. and T.P. Burt (Editors). Wiley, Chichester, Chapter 14.

Fread, D.L., 1993. In: *Handbook of Applied Hydrology*, Maidment, D.R. (Editor). McGraw-Hill, New York, Chapter 10.

Ho, L.T.K., M. Umitsu, and Y. Yamaguchi, 2010. Flood Hazard Mapping by Satellite Images and SRTM DEM in the Vu Gia–Thu Bon Alluvial Plain, Central Vietnam. *International Archives of the Photogrammetry, Remote Sensing and Spatial Information Science* 38(Part 8): 275-280.

Hollyday, E.F.,1976. Improving Estimates of Streamflow Characteristics by Using Landsat-1 Imagery. *U. S. Geological Survey, Journal of Research* 4: 517-531.

Horritt, M.S. and P.D. Bates, 2001. Predicting Floodplain Inundation: Raster-based Modelling versus the Finite-Element Approach. *Hydrological Processes* 15(5): 825-842. DOI: 10.1002/hyp.188

Hunter, N.M., P.D. Bates, M.S. Horritt, and M.D. Wilson, 2007. Simple Spatially-distributed Models for Predicting Flood Inundation: A Review. *Geomorphology* 90(3): 208-225. DOI: 10.1016/j.geomorph.2006.10.021

Interagency Advisory Committee on Waster Data (IACWD), 1982. Guidelines for Determining Flood Flow Frequency. *Bulletin 17B of the Hydrology Subcommittee*. Office of Water Data Coordination, U.S. Geological Survey, Reston, VA.

Kail, J., B. Guse, J. Radinger, M. Schröder, J. Kiesel, et al., 2015. A Modelling Framework to Assess the Effect of Pressures on River Abiotic Habitat Conditions and Biota. *PloS one* 10(6): e0130228. DOI: 10.1371/journal.pone.0130228

Kenney, T.A., and M.L. Freeman, 2011. Two-dimensional Streamflow Simulations of the Jordan River, Midvale and West Jordan, Utah. US Geological Survey Scientific Investigations Report 2011-5043. https://pubs.er.usgs.gov/publication/sir20115043

Khan, S.I., Y. Hong, J. Wang, K.K. Yilmaz, J.J. Gourley, R.F. Adler, et al., 2011. Satellite Remote Sensing and Hydrologic Modeling for Flood Inundation Mapping in Lake Victoria

Basin: Implications for Hydrologic Prediction in Ungauged Basins. *IEEE Transactions on Geoscience and Remote Sensing* 49(1): 85-95. DOI: 10.1109/TGRS.2010.2057513

Ku, Y.H. and Y.D. Kim, 2014. Comparison of Two-dimensional Model for Inundation Analysis in Flood Plain Area. *Journal of Wetlands Research* 16(1): 93-102. DOI: 10.17663/JWR.2014.16.1.093

Lane, S.N., K.F. Bradbrook, K.S. Richards, P.A. Biron, and A.G. Roy, 1999. The Application of Computational Fluid Dynamics to Natural River Channels: Three-Dimensional versus Two-dimensional Approaches. *Geomorphology* 29(1): 1-20. DOI: 10.1016/S0169-555X(99)00003-3

Lin, P., M.A.Rajib, Z.L.Yang, M. Somos-Valenzuela, V. Merwade, D.R.Maidment, et al., 2017. Spatiotemporal Evaluation of Simulated Evapotranspiration and Streamflow over Texas using the WRF-Hydro-RAPID Modeling Framework. *Journal of the American Water Resources Association (JAWRA)* 1-15. DOI: 10.1111/1752-1688.12585

Liu Y.Y., D.R. Maidment, D.G. Tarboton, et al., 2016. A Cybergis Approach to Generating High-resolution Height Above Nearest Drainage (HAND) Raster for National Flood Mapping. CyberGIS Center Technical Report: CYBERGIS-TR-2016-005-i

Maidment, D.R., 2017. Conceptual Framework for the National Flood Interoperability Experiment. *Journal of the American Water Resources Association* 53(2): 245-257. DOI: 10.1111/1752-1688.12474

Maidment, D.R., and D. Djokic, 2000. Hydrologic and Hydraulic Modeling Support: With Geographic Information Systems. Environmental Systems Research Institute, Inc. (ESRI); Redlands, CA. ISBN-13: 978-1879102804

McDonald, R.R., J.P. Bennett, and J.M. Nelson, 2001. The USGS Multi-dimensional Surface Water Modeling System. In *Proceedings, 7th US Interagency Sedimentation Conference,* Reno, Nev., p. I-161-I-167.

McDonald, R.R., J.M. Nelson, P.J. Kinzel, and J. Conaway, 2005. Modeling Surface-water Flow and Sediment Mobility with the Multi-Dimensional Surface Water Modeling System (MD_SWMS). U.S. Geological Survey Fact Sheet 2005-3078. https://pubs.er.usgs.gov/publication/fs20053078

McGehee, R., L. Li, and E. Poston, 2016. The Modified HAND Method. In: *National Water Center Innovators Program Summer Institute Report*, Maidment, D.R., A. Rajib, P. Lin, and E.P. Clark (Editors). Consortium of Universities for the Advancement of Hydrologic Science, Inc. Technical Report No. 13, 122 p. DOI: 10.4211/technical.20161019

Merwade, V., F. Olivera, M. Arabi, and S. Edleman, 2008. Uncertainty in Flood Inundation Mapping: Current Issues and Future Directions. *Journal of Hydrologic Engineering* 13(7): 608-620. DOI: 10.1061/(ASCE)1084-0699(2008)13:7(608)

National Oceanic and Atmospheric Administration (NOAA), 2016. National Water Model: Improving NOAA's Water Prediction Services. http://water.noaa.gov/documents/wrn-national-water-model.pdf

Nelson, J.M., and R.R. McDonald, 1996. Mechanics and Modeling of Flow and Bed Evolution in Lateral Separation Eddies. *USGS Director's Approved report submitted to the USGS Grand Canyon Monitoring and Research Center*. http://www. gcmrc. gov/library/reports/GCES/Physical/hydrology/Nelson1996.pdf

Nelson, J.M., J.P. Bennett, and S.M. Wiele, 2003. Flow and Sediment-transport Modeling. *Tools in Fluvial Geomorphology* 18: 539-576.

Nelson, J.M., Y. Shimizu, T. Abe, K. Asahi, M. Gamou, et al., 2016. The International River Interface Cooperative: Public Domain Flow and Morphodynamics Software for Education and Applications. *Advances in Water Resources* 93: 62-74.

National Flood Insurance Program (NFIP), 2002. National Flood Insurance Program Description. Federal Emergency Management Agency. http://www.fema.gov/library/viewRecord.do?id=1480.

Nobre, A.D., L.A. Cuartas, M. Hodnett, C.D. Rennó, G. Rodrigues, A. Silveira, et al., 2011. Height Above the Nearest Drainage – A Hydrologically Relevant New Terrain Model. *Journal of Hydrology* 404.1: 13-29. DOI: 10.1016/j.jhydrol.2011.03.051

Nobre, A.D., L.A. Cuartas, M.R. Momo, D.L. Severo, A.Pinheiro, and C.A. Nobre, 2016. HAND Contour: A New Proxy Predictor of Inundation Extent. *Hydrological Processes* 30(2): 320-333. DOI: 10.1002/hyp.10581

Noman, N. S., E. J. Nelson, and A. K. Zundel, 2001. Review of Automated Floodplain Delineation from Digital Terrain Models. *Journal of Water Resource Planning and Management* 127(6): 394–402.

Pielke, R.A., M.W. Downton, and J.B. Miller, 2002. Flood Damage in the United States, 1926-2000: A Reanalysis of National Weather Service Estimates. Boulder, CO: University Corporation for Atmospheric Research.

Priestnall, G., J. Jaafar, and A. Duncan, 2000. Extracting Urban Features from Lidar Digital Surface Models. *Computers, Environment and Urban Systems* 24(2): 65-78. DOI: 10.1016/S0198-9715(99)00047-2

Rango, A., J. Foster, and V.V. Salomonson, 1975. Extraction and Utilization of Space Acquired Physiographic Data for Water Resources Development. *Journal of the American Water Resources Association* 11(6): 1245-1256. DOI: 10.1111/j.1752-1688.1975.tb01846.x

Romanowicz, R., K.J. Beven, J. Tawn, 1996. Bayesian Calibration of Flood Inundation Models. In: *Floodplain Processes*, Anderson, M.G., D.E. Walling, and P.D. Bates (Editors). Wiley, Chichester, pp. 333-360.

Rennó, C.D., A.D. Nobre, L.A. Cuartas, J.V. Soares, M.G. Hodnett, J. Tomasella, et al., 2008. HAND, A New Terrain Descriptor using SRTM-DEM: Mapping Terra-firme Rainforest Environments in Amazonia. *Remote Sensing of Environment* 112(9): 3469-3481. DOI: 10.1016/j.rse.2008.03.018

Shalaby, A. and R. Tateishi, 2007. Remote Sensing and GIS for Mapping and Monitoring Land Cover and Land-use Changes in the Northwestern Coastal Zone of Egypt. *Applied Geography* 27(1): 28-41. DOI: 10.1016/j.apgeog.2006.09.004

Smith, L. C., 1997. Satellite Remote Sensing of River Inundation Area, Stage, and Discharge: A Review. *Hydrological processes* 11(10): 1427-1439. DOI: 10.1002/(SICI)1099-1085(199708)11:10<1427::AID-HYP473>3.0.CO;2-S

Sollers, S. C., A. Rango, and D.L. Henninger, 1978. Selecting Reconnaissance Strategies for Floodplain Surveys. *Journal of the American Water Resources Association* 14(2): 359-373. DOI: 10.1111/j.1752-1688.1978.tb02173.x

Son, G., H. You, and D. Kim, 2014. Feasibility Calculation of FaSTMECH for 2D Velocity Distribution Simulation in Meandering Channel. *Journal of the Korean Society of Civil Engineers* 34(6): 1753-1764. DOI: 10.12652/Ksce.2014.34.6.1753

White F., 1974. Viscous Fluid Flow. McGraw-Hill, New York, ISBN-13: 978-1259002120

Zhang, J., D. Munasinghe, and Y.F. Huang, 2016. Comparison of Flood Inundation Mapping Techniques between Different Modeling Approaches and Satellite Imagery. In: *National Water Center Innovators Program Summer Institute Report*, Maidment, D.R., A. Rajib, P. Lin, and E.P. Clark (Editors). Consortium of Universities for the Advancement of Hydrologic Science, Inc. Technical Report No. 13, 122 p. DOI: 10.4211/technical.20161019

Table 1. Comparison of dynamic-based and terrain-based inundation approaches

Model Type		Reference	Routing	Data requirement	Run time	Calibration	Validation
Dynamic-based	1D	Fread (1984); Fread (1993)	Full solution of the 1D St. Venant equations	Discharge, DEM, Cross-sections, Channel parameters, Land use/type	Fast	Necessary	Yes
	2D	Bates *et al*. (1992)	Full solution of the 2D St. Venant equations with turbulence closure	Discharge, DEM, Land use/type	Moderate	Contingent	Yes
	3D	White (1974); Lane *et al*. (1999)	Full solution of the Navier-Stokes equations	3D DEM, 3D bathymetry, 3D velocity, Land use/type	Slow	Contingent	Yes
Terrain-based	Planar water surface	Priestnall *et al*.(2000)	None	DEM, water surface elevation	Fast	Limited	Yes
	Storage cell	Cunge *et al*. (1976); Estrela (1994); Romanowicz *et al*.	Uniform flow formula (Manning equation or weir-type equations);	DEM, discharge, Initial channel flow depth, Land	Fast	Limited	Yes

		(1996); Bates and De Roo (2000);	Kinematic wave and Manning equation	use/type			
	HAND	Nobre *et al*. (2011)	Uniform flow formula (Manning equation)	DEM, discharge/water surface elevation, Land use/type	Fast	Limited	Yes

Table 2. iRIC model settings

Setting Menu	Description
Initial Condition	Initial Water Surface Elevation: 1D step-backwater
Boundary Condition	Downstream Peak Discharge: 4445.7 m^3/s
	Downstream Peak Stage: 49.7 m
Iteration	1500
Upstream Discharge	4300 m^3/s
Upstream Stage	Constant (time-invariant)
Drag Coefficient	Variable
Re-wetting	On

FIGURE CAPTIONS

Figure 1. The study area and stream reaches in the Brazos River, Texas

Figure 2. Satellite imageries showing A. pre-flood (12 p.m. on March 25th, 2016(CDT)) and B. post-flood condition (12 p.m. on May 28th, 2016(CDT)) in the study area

Figure 3. Stage hydrograph and rainfall hyetograph shows the target timing of model simulation and the timing of satellite observation

Figure 4. Schematic diagram of this study

Figure 5. U.S. Geological Survey gage observed hydrograph and the National Water Model hydrograph with nudging-based data assimilation

Figure 6. Results of inundation maps and fitness indices from simulation of (A) HAND, (B) iRIC, (C) Modified HAND, and (D) Satellite Observation

Figure 7. (A) Inundation map derived from HAND on top of DEM, (B) Cross-sectional view of the selected area and water surface simulated in HAND, (C) Inundation map derived from the modified HAND on top of DEM, (D) Cross-sectional view of the selected area and water surface simulated in modified HAND

Figure 1

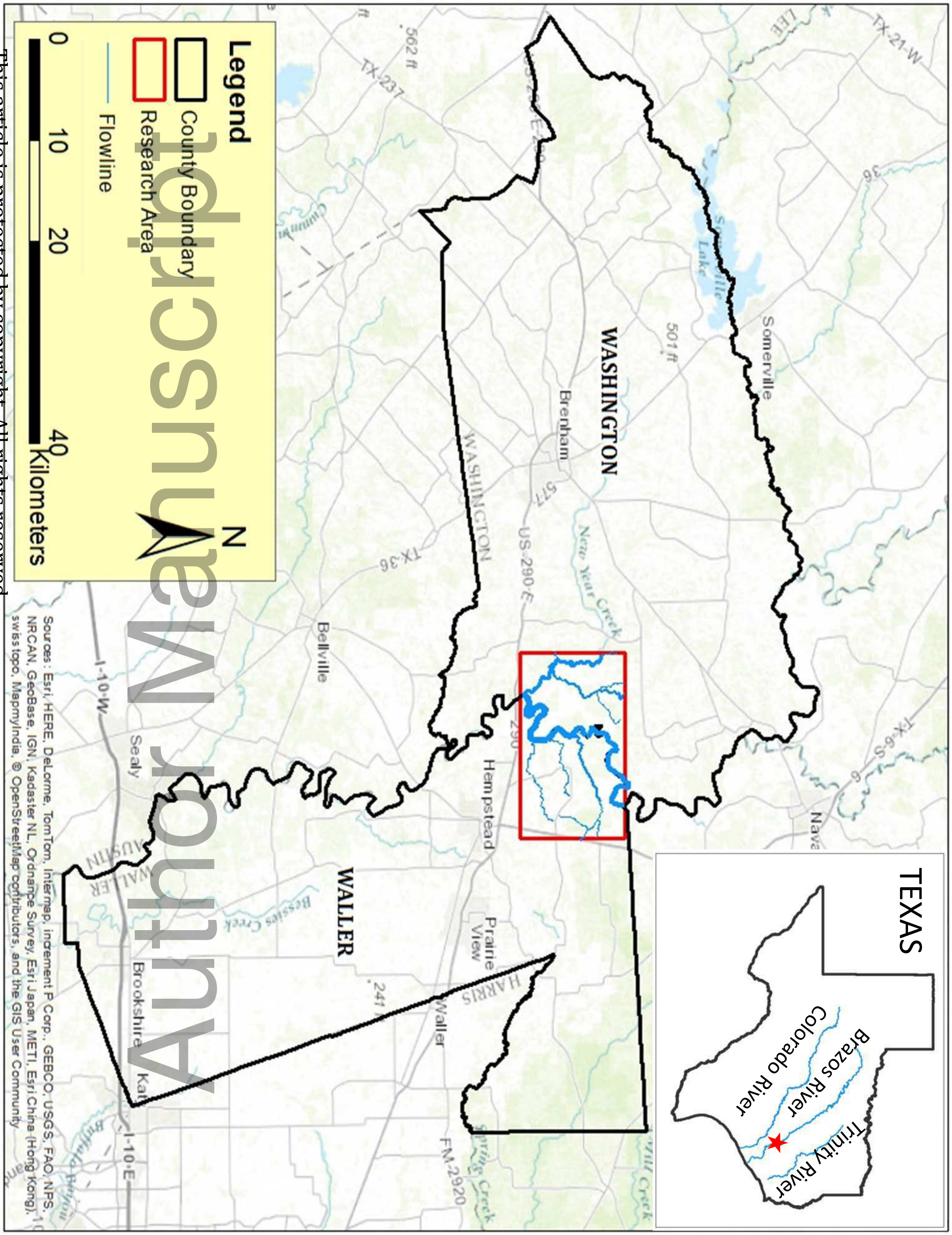

Legend
County Boundary
Research Area
Flowline
0
10
20
40
Kilometers
N
WASHINGTON
WALLER
Brenham
Somerville
Hempstead
Bellville
Sealy
Prairie View
Waller
Brookshire
New Year Creek
US-290-E
TX-36
I-10-W
I-10-E
FM-2920
TEXAS
Colorado River
Brazos River
Trinity River
Sources: Esri, HERE, DeLorme, TomTom, Intermap, increment P Corp., GEBCO, USGS, FAO, NPS, NRCAN, GeoBase, IGN, Kadaster NL, Ordnance Survey, Esri Japan, METI, Esri China (Hong Kong), swisstopo, MapmyIndia, © OpenStreetMap contributors, and the GIS User Community

Figure 2

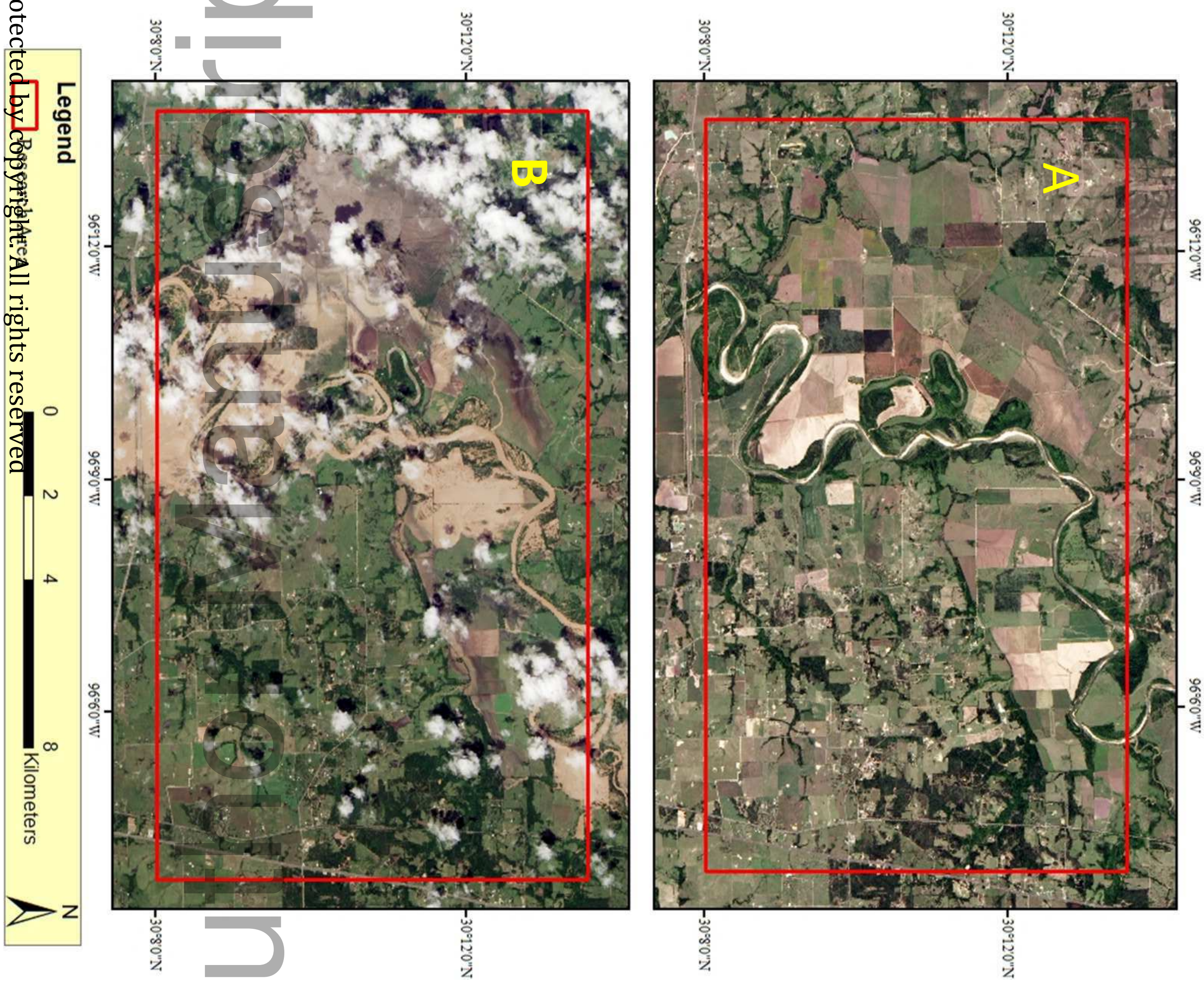

A
B
30°12'0"N
30°8'0"N
96°12'0"W
96°9'0"W
96°6'0"W
Legend
0
2
4
8
Kilometers
N

Figure 3

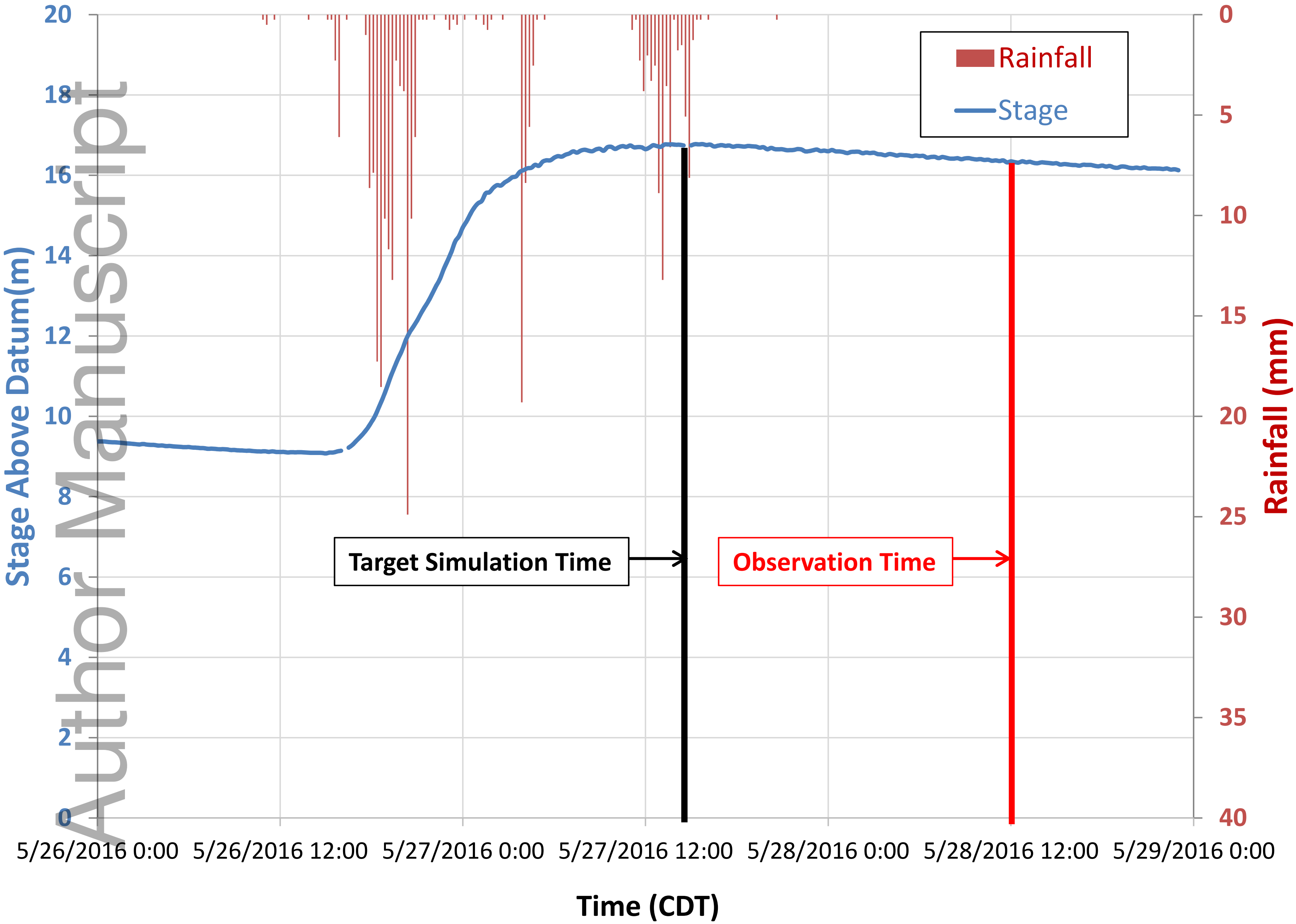

Rainfall
Stage
Stage Above Datum(m)
Rainfall (mm)
20
18
16
14
12
10
8
6
4
2
0
5
10
15
20
25
30
35
40
Target Simulation Time
Observation Time
5/26/2016 0:00
5/26/2016 12:00
5/27/2016 0:00
5/27/2016 12:00
5/28/2016 0:00
5/28/2016 12:00
5/29/2016 0:00
Time (CDT)

Figure 4

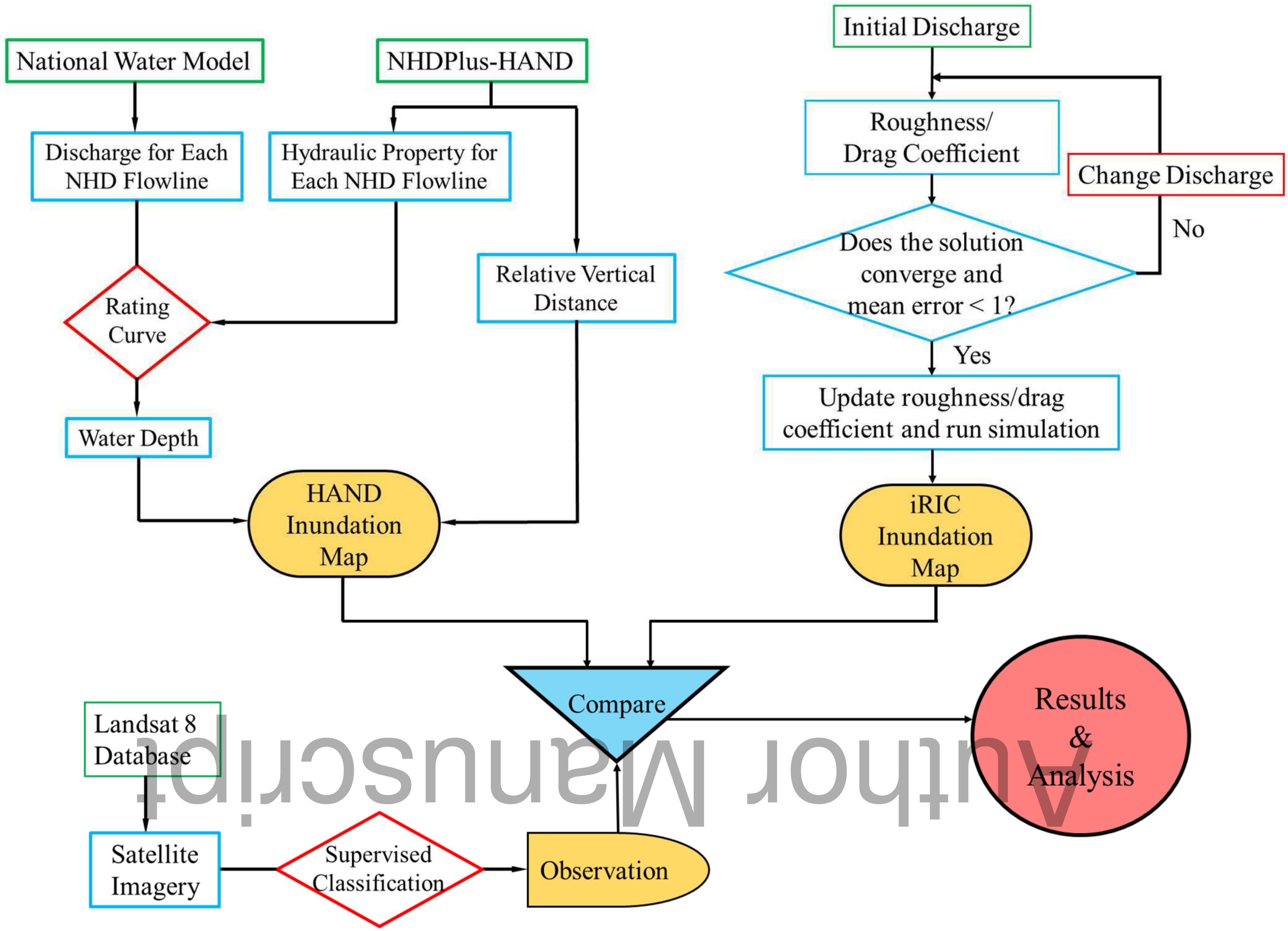

National Water Model
NHDPlus-HAND
Initial Discharge
Discharge for Each NHD Flowline
Hydraulic Property for Each NHD Flowline
Roughness/ Drag Coefficient
Change Discharge
No
Relative Vertical Distance
Does the solution converge and mean error < 1?
Rating Curve
Yes
Update roughness/drag coefficient and run simulation
Water Depth
HAND Inundation Map
iRIC Inundation Map
Compare
Results & Analysis
Landsat 8 Database
Satellite Imagery
Supervised Classification
Observation

Figure 5

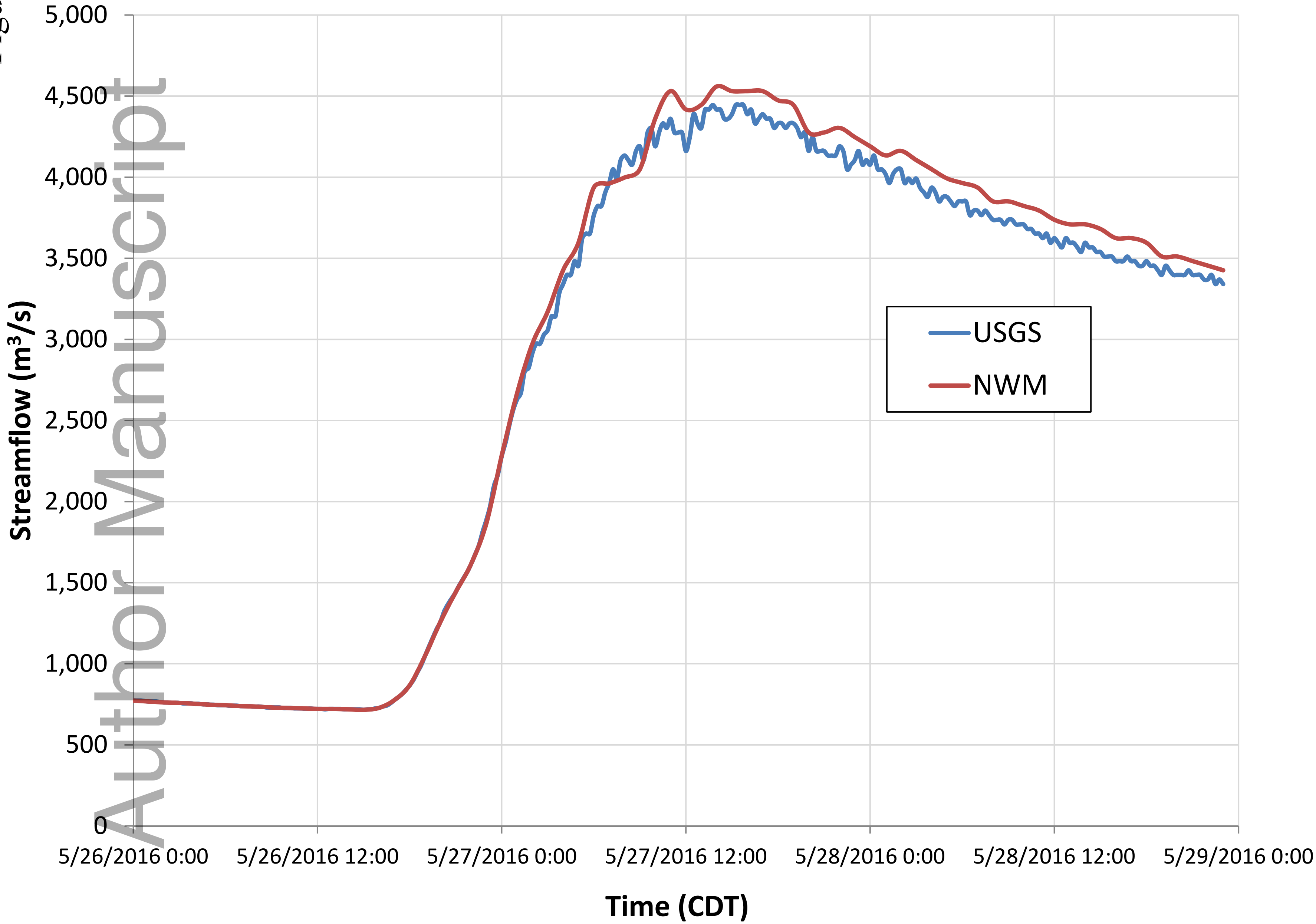
5,000
4,500
4,000
3,500
3,000
2,500
2,000
1,500
1,000
500
0
Streamflow (m³/s)
5/26/2016 0:00
5/26/2016 12:00
5/27/2016 0:00
5/27/2016 12:00
5/28/2016 0:00
5/28/2016 12:00
5/29/2016 0:00
Time (CDT)
USGS
NWM

Figure 6

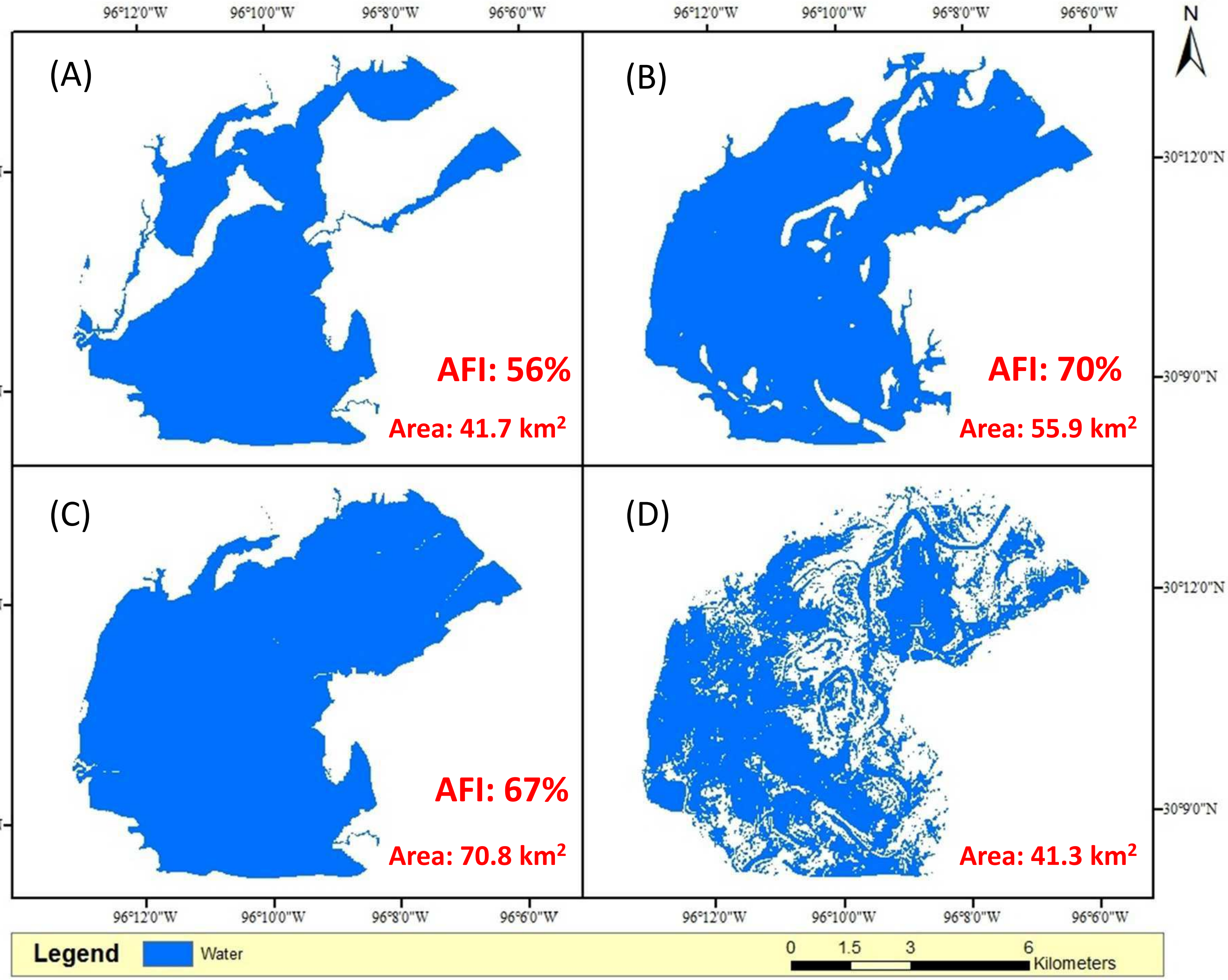
(A)
AFI: 56%
Area: 41.7 km²
(B)
AFI: 70%
Area: 55.9 km²
(C)
AFI: 67%
Area: 70.8 km²
(D)
Area: 41.3 km²
96°12'0"W
96°10'0"W
96°8'0"W
96°6'0"W
30°12'0"N
30°9'0"N
N
Legend
Water
0
1.5
3
6
Kilometers

Figure 7

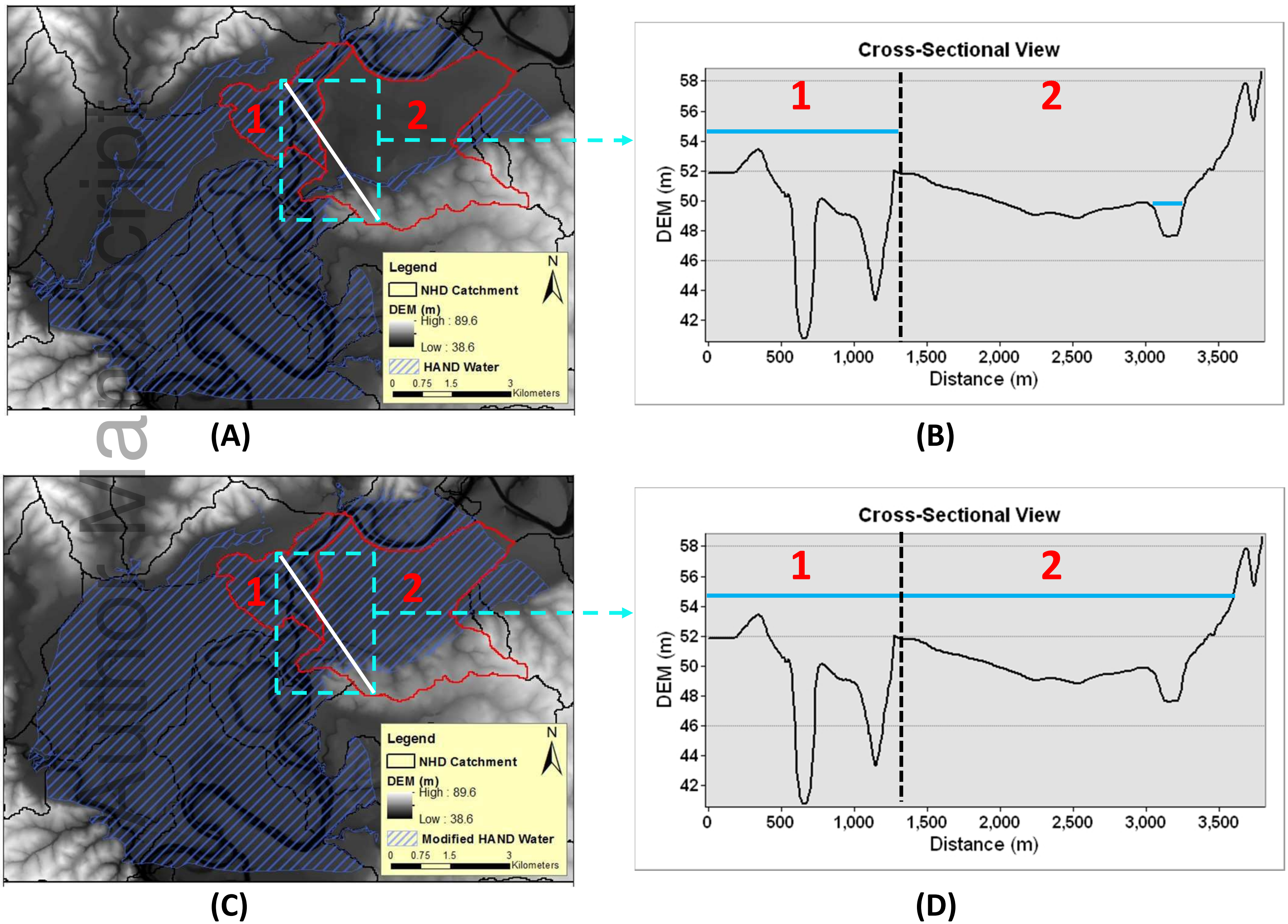
1
2
Legend
N
NHD Catchment
DEM (m)
High : 89.6
Low : 38.6
HAND Water
0 0.75 1.5 3 Kilometers
(A)
Cross-Sectional View
1
2
DEM (m)
Distance (m)
58
56
54
52
50
48
46
44
42
0 500 1,000 1,500 2,000 2,500 3,000 3,500
(B)
1
2
Legend
N
NHD Catchment
DEM (m)
High : 89.6
Low : 38.6
Modified HAND Water
0 0.75 1.5 3 Kilometers
(C)
Cross-Sectional View
1
2
DEM (m)
Distance (m)
58
56
54
52
50
48
46
44
42
0 500 1,000 1,500 2,000 2,500 3,000 3,500
(D)